Polymer 51 (2010) 5407–5416

Contents lists available at ScienceDirect

Polymer

journal homepage: www.elsevier.com/locate/polymer

# Synthesis and alkaline stability of novel cardo poly(aryl ether sulfone)s with pendent quaternary ammonium aliphatic side chains for anion exchange membranes

Qiang Zhang [a,b], Qifeng Zhang [a,b], Junhua Wang [a,b], Suobo Zhang [a,*], Shenghai Li [a]

[a] *Key Laboratory of Advanced Ecomaterials, Changchun Institute of Applied Chemistry, Chinese Academy of Sciences, Changchun 130022, China*
[b] *Graduate School of Chinese Academy of Sciences, Beijing 100049, China*

ARTICLE INFO

*Article history:*
Received 30 May 2010
Received in revised form
14 September 2010
Accepted 16 September 2010

*Keywords:*
Anion exchange membrane
Hydroxide ion conductivity
Dimensional stability

## ABSTRACT

Novel cardo poly(aryl ether sulfone)s containing pendent $-[CH_2CH_2NMe_3]^+OH^-$, or $-[CH_2CH_2CH_2NMe_3]^+OH^-$ groups, and partially fluorinated cardo poly(aryl ether sulfone) containing pendent $-[CH_2CH_2CH_2NMe_3]^+OH^-$ groups were synthesized and examined with the focus of understanding how the polymer chemical structure affects their morphology, ion conductivity and alkaline stability. The resulting quaternized polymers exhibited outstanding solubility in polar aprotic solvents. The partially fluorinated cardo poly(aryl ether sulfone)s (PES-PF-OH) with ion-exchange capacity of 1.44 meq $g^{-1}$ displayed the highest ion conductivities, varied from $3.0 \times 10^{-2}$ to $4.1 \times 10^{-2}$ S $cm^{-1}$ over the range 20–60 °C. TEM revealed that PES-PF-OH membrane exhibited a distinct phase-separated morphology comprised of interconnected ionic clusters in size of 1–2 nm. The studies on alkaline stability of the membranes revealed that the PES-PF-OH polymer was not stable under strong basic conditions. The quarternized polymers containing pendent $-[CH_2CH_2NMe_3]^+OH^-$, or $-[CH_2CH_2CH_2NMe_3]^+OH^-$ groups mainly underwent Hofmann elimination and $S_N2$ substitution reaction.

## 1. Introduction

Ion-conducting polymers are of interest for a variety of applications, such as sensors, actuators, batteries, and ion-exchange membranes or resins. In recent years, studies on ion-conducting polymers have been strongly promoted as a result of a considerable interest in the development of high performance polymer electrolyte membrane fuel cells for transportation, stationary and portable power applications [1–3]. Polymer electrolyte membrane fuel cells (PEMFCs) based on proton exchange membrane (PEM), especially Nafion membrane, have been intensively studied [4]. It has been recognized that some specific limitations exist for PEMFCs, including slow electrode-kinetics, CO poisoning of Pt and Pt-based electrocatalysts at low temperatures, and high cost of the membrane and catalyst. In view of this, alkaline anion exchange membrane fuel cells (AEMFCs) have attracted much attention since it has many attractive advantages over PEM fuel cell, including performance and cost. The faster kinetics of oxygen reduction reactions in alkaline media allows the use of nonprecious metal electrocatalysts, thus drastically reducing the cost of the fuel cell [5]. Furthermore, ion transport within the membrane is from the cathode to the anode, opposing the direction of methanol crossover from anode to cathode, which will reduce the methanol permeability. Challenges in the development of AEMFCs include the development of stable anion exchange membranes (AEMs) at high pH. The commercial membranes containing substituted polystyrene are not stable in basic medium. For the design of novel AEMs, aromatic ionomers are the preferred candidates for fuel cell applications due to their excellent thermal and mechanical properties as well as their resistance to oxidation and stability in acidic and alkaline conditions. Chloromethyl groups can be introduced onto the phenyl ring of the aromatic backbone via the chloromethylation reaction. Subsequently, the AEMs are prepared by amination of chloromethlated polymers with various amines. Using this general method, polysulfones containing quaternary ammonium [6–8], guanidinium [9] and quaternary phosphonium groups [10] have been prepared and evaluated for the application in AEMFCs. However, chloromethylation reaction is usually restricted due to their lack of precise control over the degree and location of functionalization [6,11] and the use of a toxic regent, chloromethyl methyl ether [12,13].

---

* Corresponding author. Tel.: +86 431 5605139.
*E-mail address:* sbzhang@ciac.jl.cn (S. Zhang).

0032-3861/$ – see front matter © 2010 Elsevier Ltd. All rights reserved.
doi:10.1016/j.polymer.2010.09.049

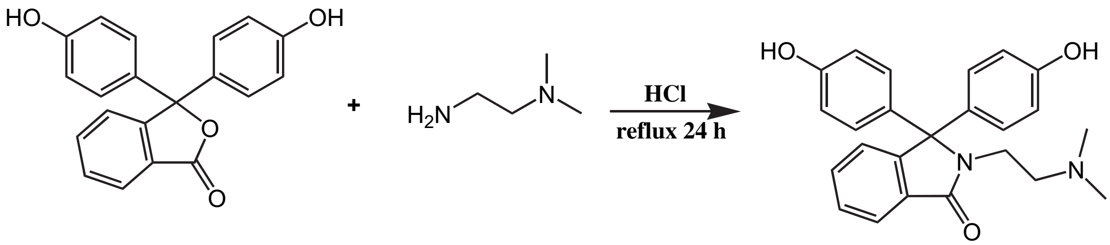

**Scheme 1.** The synthetic route of monomer PPH-DMEA.

A strategy to improve the stability and conductivity of aromatic ionomers is to distinctly separate the hydrophilic functional groups from the hydrophobic polymer main chain by, e.g., locating the sulfonic acid groups on side chains grafted onto the polymer main chain [14–16]. Most of the sulfonated proton exchange membranes were obtained by post-sulfonation process and direct polymerization from sulfonated monomers to introduce sulfonic acid group to polymer side chain, while aromatic ionomer containing quaternary ammonium aliphatic side chains was seldom achieved probably due to the lack of appropriate and commercially available monomers and convenient approach to convert them into anion-conductive materials.

In this study, a series of novel cardo poly(aryl ether sulfone)s containing pendent $-[CH_2CH_2NMe_3]^+OH^-$, or $-[CH_2CH_2CH_2NMe_3]^+OH^-$ groups, and partially fluorinated cardo poly(aryl ether sulfone) containing pendent $-[CH_2CH_2CH_2NMe_3]^+OH^-$ groups were synthesized. The tertiary monomers were easily prepared by the reaction of phenolphthalein with commercially available N,N-dimethyl-1,3-propanediamine (DMPA) or N,N-dimethylethane-1,2-diamine (DMEA). With these monomers, cardo poly(aryl ether sulfone)s with pendent tertiary amine groups were then prepared. Alkaline anion exchange membranes were made by the reaction of the tertiary amine groups with iodomethane to form quaternary ammonium groups which acted as the counterion for hydroxide anion. An advantage of this method is avoiding the use of toxic chloromethylation reagents. Their properties, such as the solubility, thermal stability, mechanical strength, water uptake behavior, hydroxide ion conductivity, area resistance, static transport number, morphology, and alkaline stability have been investigated in detail.

## 2. Experimental part

### 2.1. Materials and chemicals

Phenolphthalein (PPH) was purchased from Beijing Chemical Reagent Company, and purified by recrystallization from mixed solvent of ethanol and water. 4,4′-dichlorodiphenylsulfone (DCDPS), N,N-dimethyl-1,3-propanediamine (DMPA), N,N-dimethylethane-1,2-diamine (DMEA) and iodomethane were purchased from Aldrich and used as received. Dimethylsulfoxide (DMSO) and N-Methyl-2-pyrrolidinone (NMP) were firstly dried over $CaH_2$ and then distilled under reduced pressure before use. All other reagents were obtained from commercial sources and used as received.

#### 2.1.1. Synthesis of 2-(3-(dimethylamino)propyl)-3,3′-bis(4-hydroxyphenyl)isoindolin-1-one (PPH-DMPA)

The monomer PPH-DMPA was prepared according to the previously reported method [17]. Yield: 85%. mp: 236.0–237.0 °C. 9.55 (2H, s), 7.65–7.68 (1H, d), 7.49–7.54 (1H, t), 7.43–7.45 (1H, t), 7.39–7.41 (1H, d), 6.91–6.94 (4H, d), 6.70–6.73 (2H, d), 1.91 (6H, s), 0.84–0.91(2H, m), FT-IR (KBr): 3201 $cm^{-1}$ (O–H), 2963 $cm^{-1}$ ($\upsilon_{C-H}$), 1685 $cm^{-1}$ (C=O of phthalimidine).

#### 2.1.2. Synthesis of 2-(2-(dimethylamino)ethyl)-3,3′-bis(4-hydroxyphenyl)isoindolin-1-one (PPH-DMEA)

The monomer PPH-DMEA was prepared according to the previously reported method [18]. Mp: 264.5–265.5 °C, the yield was 82%. $^1H$ NMR (DMSO-$d_6$-ppm): 9.58 (2H, s), 7.67–7.68 (1H, d), 7.52–7.55 (1H, t), 7.44–7.46 (1H, t), 7.39–7.41 (1H, d), 3.37–3.40 (2H, t), 6.94–6.96 (4H, d), 6.73–6.74 (2H, d), 1.91 (6H, s), 1.55–1.58 (2H, t). IR (KBr): 2963 $cm^{-1}$ ($\upsilon_{C-H}$), 1683 $cm^{-1}$ ($\upsilon_{C=O}$ of phthalimidine), 3280 $cm^{-1}$ ($\upsilon_{O-H}$)

#### 2.1.3. Synthesis of 3,3′,4,4′-tetrafluorodiphenylsulfone (TFDPS)

The monomer TFDPS was prepared by the same method reported by our group in previous paper [19].

#### 2.1.4. Synthesis of cardo poly(aryl ether sulfone)s containing pendent tertiary amine groups

Cardo poly(aryl ether sulfone)s containing $-(CH_2CH_2CH_2NMe_2)$ (PES-P-N) or $-(CH_2CH_2NMe_2)$ (PES-E-N) groups were prepared according to the previously reported method [17,18]. A typical synthetic procedure, illustrated by the preparation of PES-P-N polymer, is described as follows. Polymerizations of PPH-DMEA (3.8846 g,

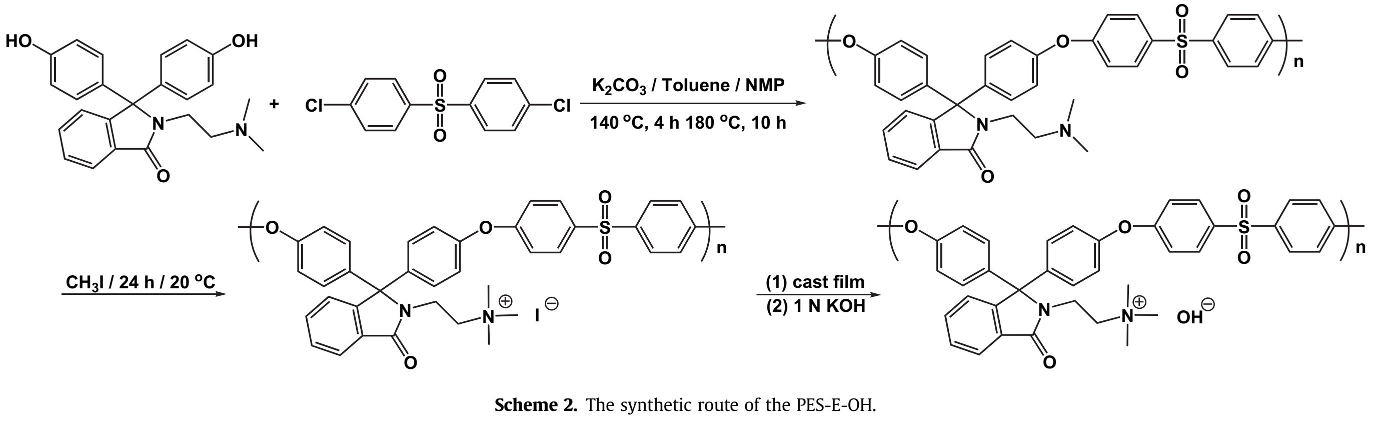

**Scheme 2.** The synthetic route of the PES-E-OH.

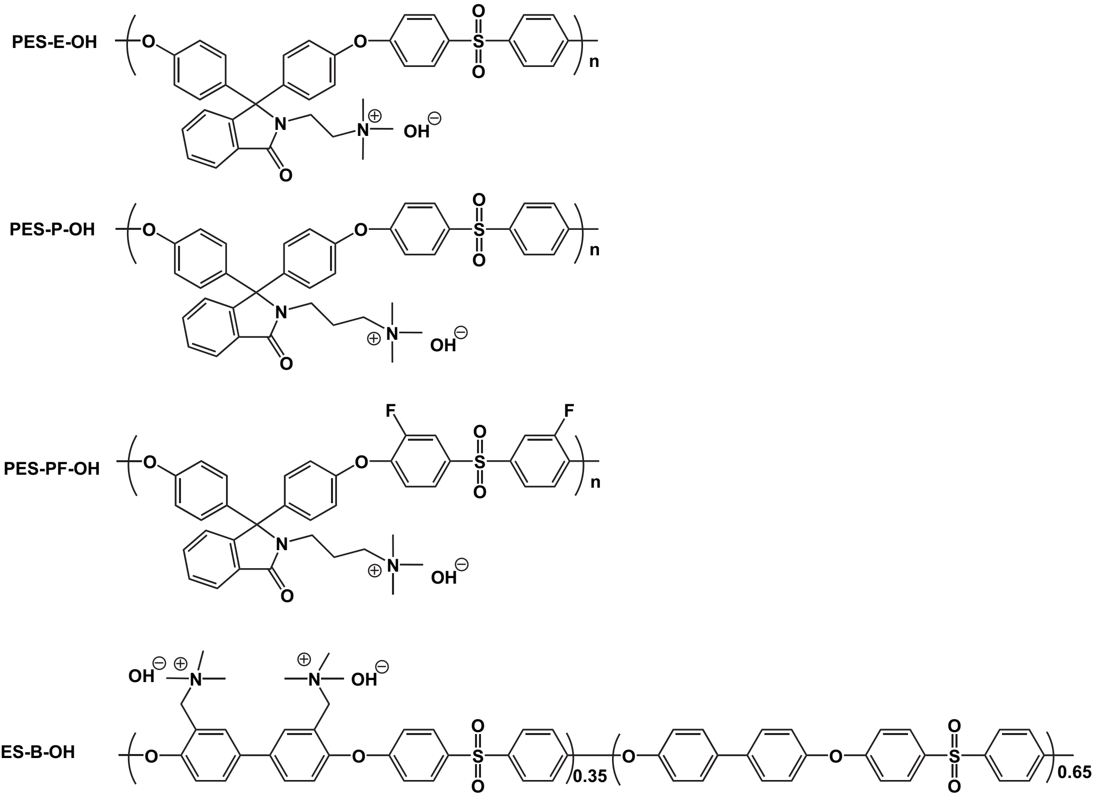

**Fig. 1.** The chemical structures of the ionomers synthesized in this study.

10 mmol) and DCDPS (2.8716 g, 10 mmol) were conducted in a flame dried three-necked flask. The flask was fitted with a nitrogen inlet, over-head stirrer and Dean Stark trap fitted with a condenser. After charging all the monomers and solvent, the reaction flask was heated in an oil bath to 140 °C while the toluene was allowed to reflux for 4 h to remove any water present from the hydrated atmosphere or hydrated monomers. The toluene was then removed over a 60 min time interval. The Dean Stark trap was emptied and the reaction temperature was slowly increased to 180 °C for 10 h. The resulting solution media became very viscous. The viscous solution was cooled to room temperature and then diluted with NMP. The polymer solution was filtered to remove the salt byproduct and then isolated by precipitation in deionized (DI) water. The resulting fibrous polymer was washed thoroughly with water several times and dried in a vacuum oven at 120 °C for 24 h. Yield: 98%.

### *2.1.5. Synthesis of partially fluorinated cardo poly(aryl ether sulfone)s containing pendent tertiary amine groups*

A flame dried 100 mL three-necked flask equipped with a nitrogen inlet and over-head stirrer was charged with PPH-DMPA (2.0125 g, 5 mmol), TFDPS (1.4512 g, 5 mmol), $K_2CO_3$ (1.38 g, 10 mmol), and dry NMP (34 mL, 10% solids). The mixture was kept at room temperature for a few minutes and then slowly heated at 90 °C for 10 h. After cooling to room temperature, an additional 30 mL of NMP was added so as to dilute the highly viscous solution, after which the solution was filtered and dropped into stirred deionized water. The fiber-like precipitate was filtered off and washed with hot water three times prior to being dried under vacuum to produce the final product. Yield: 98%.

### *2.1.6. Synthesis of cardo poly(aryl ether sulfone)s containing alkyl ammonium groups (PES-E-I, PES-P-I and PES-PF-I)*

A typical synthetic procedure, illustrated by the preparation of PES-E-I polymer, is described as follows. Iodomethane was added at a molar ratio of 2 compared to amino groups to a solution of PES-E-N in DMSO and the mixture was stirred for 24 h. The polymer solution was isolated by precipitation in deionized (DI) water, separated by filtration and dried in a vacuum oven at 120 °C for 24 h.

## *2.2. Membrane preparation*

The membranes were prepared by the dissolution of the quaternized polymers in NMP (5% w/v). The solution was then filtered

**Table 1**
Viscosity values, molecular weights and mechanical properties of membranes in dry state.

| Polymer | $\eta$ (dL$^{-1}$ g) | $M_n \times 10^3$ (g/mol) | $M_w \times 10^3$ (g/mol) | PDI | Tensile strength (MPa) | Young Modulus (GPa) | Elongation break (%) |
|---|---|---|---|---|---|---|---|
| PES-E-N | 0.50 | 41.5 | 89.7 | 2.16 | 52.9 | 1.09 | 10.6 |
| PES-E-OH | 1.20 | 54.0 | 125.6 | 2.33 | 34.8 | 0.59 | 33.9 |
| PES-P-N | 0.44 | 40.7 | 91.0 | 2.24 | 50.2 | 1.08 | 12.5 |
| PES-P-OH | 1.13 | 52.9 | 127.4 | 2.42 | 31.9 | 0.54 | 31.7 |
| PES-PF-N | 0.52 | 50.3 | 92.0 | 1.83 | 60.0 | 1.94 | 17.9 |
| PES-PF-OH | 1.15 | 70.4 | 138.0 | 1.96 | 48.3 | 0.86 | 23.8 |

Samples were dried at ambient conditions for 1 day and tested at 30 °C, 30% RH.

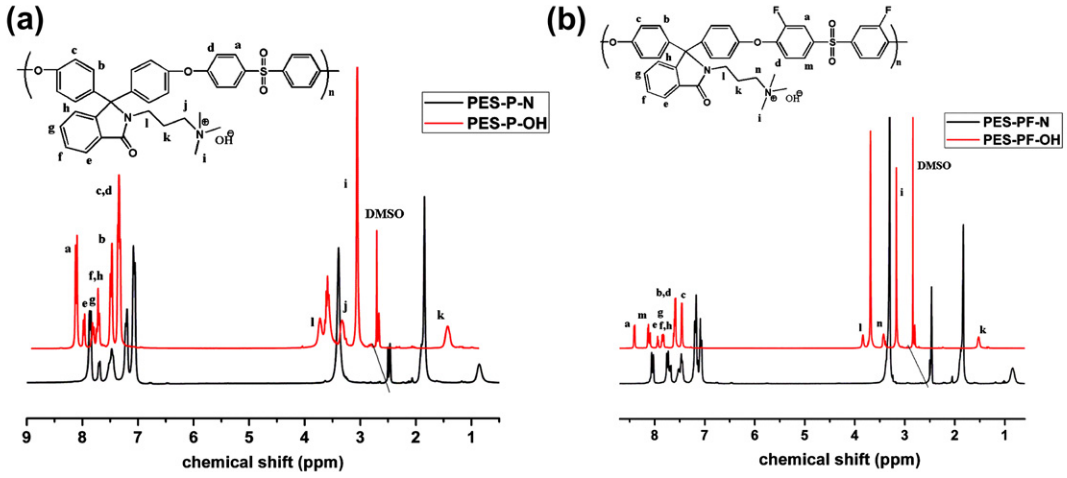

**Fig. 2.** $^1$H NMR spectra of PES-P-N and PES-P-OH (a), PES-PF-N and PES-PF-OH (b) in DMSO.

through a 0.45 μm Teflon syringe filter and cast onto a clean glass substrate. The membranes were slowly dried in an oven for 12 h at 80 °C and then in vacuo at 100 °C for 24 h, forming thin films about 30 μ thick after complete evaporation of the organic solvent.

The above quaternized membranes were soaked in 1.0 M potassium hydroxide aqueous solution at room temperature for 48 h, followed by washing with deionized water several times and soaking in deionized water with many times exchanges within 48 h prior to evaluation.

### 2.3. *Characterization*

Nuclear magnetic resonance (NMR) spectra were recorded using a Varian Unity Inova spectrometer at a resonance frequency of 400 MHz for $^1$H NMR and 376 MHz for $^{19}$F NMR in DMSO-$d_6$. The chemical shifts relative to tetramethylsilane for $^1$H NMR and fluorobenzene for $^{19}$F NMR are reported on the ppm scale. Attenuated total reflectance infrared (ATR-IR) characterization of the membranes surface was made with a Bio-Rad digilab Division FST-80 spectrometer. Inherent viscosities of all polymers were determined at 30 ± 0.1 °C using Ubbelodhe viscometer with 0.5 dL/g concentration in NMP. Molecular weight measurement was performed via gel permeation chromatography with JASCO PU-2080 Plus with two polystyrene gel column (TSK GELs; GMH$_{HR}$-M). N,N-dimethylformamide (DMF) containing 0.01 M LiBr was used as a solvent at a flow rate of 1.0 mL/min. The thermogravimetric analyses (TGA) were obtained in nitrogen with a Perkin Elmer TGA-2 thermogravimetric analyzer (Inspiratech 2000 Ltd., UK) at a heating rate of 10 °C/min. Tensile measurement was performed with a mechanical tester Instron-1211 instrument (Instron Co., USA) at a speed of 2 mm/min at ambient humidity (~30% relative humidity). The ion-exchange capacity, defined in this study as mmol (OH$^-$) g$^{-1}$ (dry AEM), was determined using the standard back-titration technique reported previously [20]. Hydroxide anion conductivity of the membranes was measured by two-probe electrochemical impedance spectroscopy (EIS) using a Solartron 1260 frequency response analyzer coupled to a Solartron 1287 potentiostat.

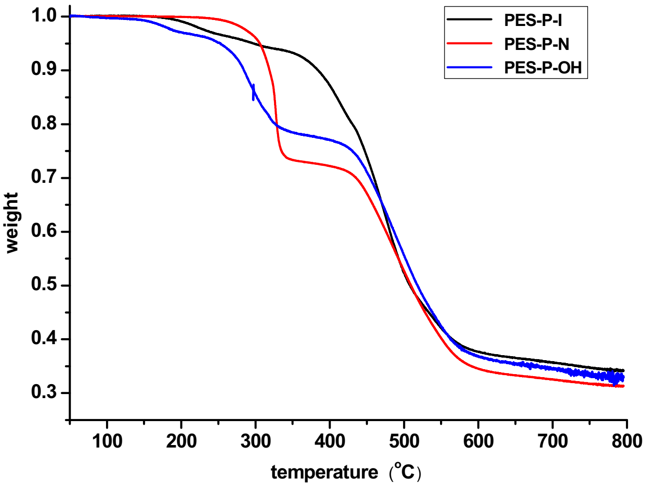

**Fig. 3.** TGA curves for PES-P-N, PES-P-I and PES-P-OH membranes in N$_2$.

#### 2.3.1. *Water uptake and swelling ratio measurements*

The membrane sample (30–40 mg per sheet) was dried at 50 °C under vacuum for 48 h until constant weight as dry material was obtained. It was immersed into deionized water at given temperature for 8 h and then quickly taken out, wiped with tissue paper, and quickly weighted on a microbalance. Use Eq. (1) to calculate the water uptake (wu):

$$\text{Water uptake}(\%) = \left[\left(W_{\text{wet}} - W_{\text{dry}}\right)/W_{\text{dry}}\right] \times 100\% \tag{1}$$

where $W_{\text{dry}}$ and $W_{\text{wet}}$ are the weight of the dry and the corresponding water-swollen membranes, respectively. The water swelling ratio of the membranes was investigated by immersing the round-shaped samples into water at room temperature for a given time, and the swelling ratio (sr) was calculated from:

$$\text{Swelling ratio}(\%) = \left[\left(l_{\text{wet}} - l_{\text{dry}}\right)/l_{\text{dry}}\right] \times 100\% \tag{2}$$

Here, $l_{\text{dry}}$ and $l_{\text{wet}}$ are the length of the dry and wet samples, respectively.

**Table 2**
IEC, water uptake and swelling ratio of membranes.

| Polymer | IEC (meq g$^{-1}$) | | Water uptake (%) | | Swelling ratio (%) | |
|---|---|---|---|---|---|---|
| | Theoretical | Experimental | 20 °C | 60 °C | 20 °C | 60 °C |
| PES-E-N | | | 5.7 | 7.2 | 3.0 | 3.9 |
| PES-E-OH | 1.57 | 1.52 | 25.8 | 27.5 | 4.2 | 5.5 |
| PES-P-N | | | 5.5 | 6.9 | 3.1 | 3.8 |
| PES-P-OH | 1.54 | 1.50 | 25.1 | 28.3 | 4.2 | 5.4 |
| PES-PF-N | | | 3.0 | 4.4 | 0 | 1 |
| PES-PF-OH | 1.46 | 1.44 | 15.1 | 18.4 | 2.7 | 3.0 |
| PES-B-OH | 1.50 | 1.51 | 20.0 | 22.7 | 4.0 | 4.2 |

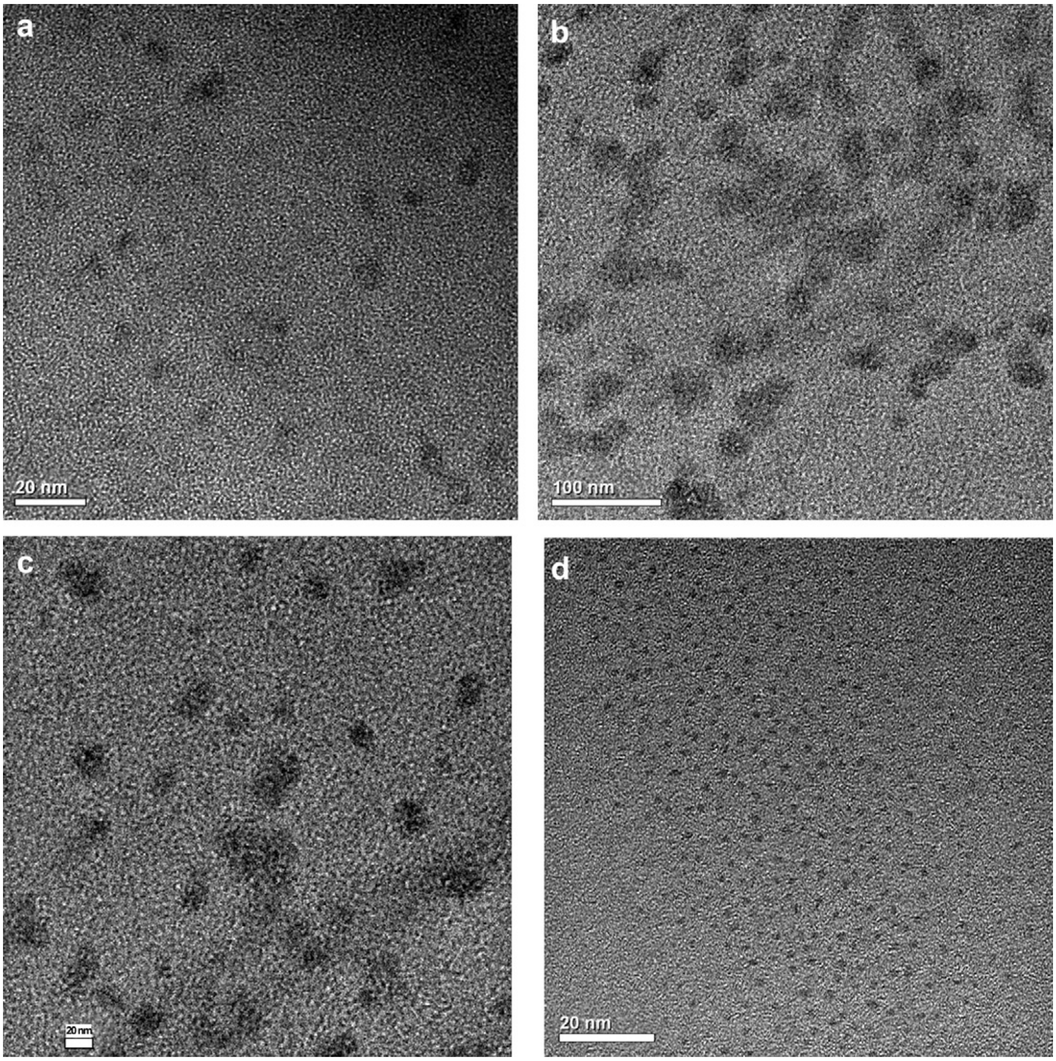

**Fig. 4.** TEM micrographs of polymer membranes: (a) PES-B-OH, (b); (c) PES-P-OH and (d) PES-PF-OH.

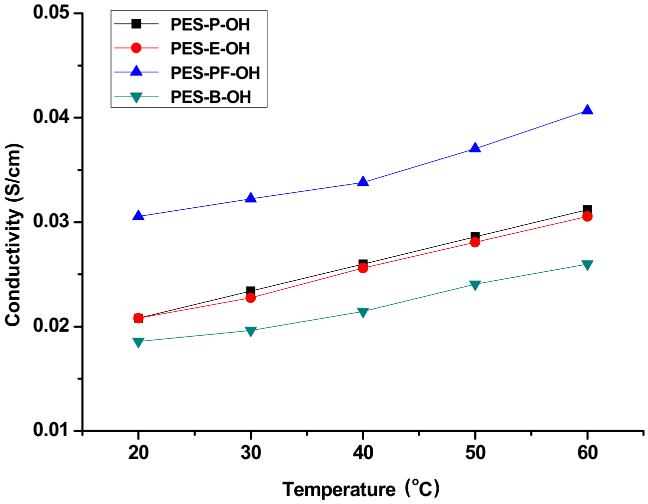

**Fig. 5.** Temperature dependence of the hydroxide ion conductivities of PES-E-OH, PES-P-OH, PES-PF-OH and PES-B-OH membranes.

### *2.3.2. Transmission electron microscopy*

In order to obtain TEM images, the membrane was first dyed with $PdCl_4^{2-}$ by immersing in a $PdCl_4^{2-}$/HCl solution for 2 days, and then rinsed with excessive water and finally dried at room temperature for 12 h. The dyed sample was embedded in epoxy resin and sectioned using a microtome to yield a 50 nm thick sample which was placed on copper grids. Images were taken on an ultrahigh-resolution transmission electron microscope (JEOLJEM-2010FEF) using an accelerating voltage of 200 kV.

### *2.3.3. Membrane area resistance and the transport number*

The measurement of membrane area resistance and the transport number was based on the procedure in the literature [21] with a few modifications. The area resistance was measured in

**Table 3**
Area resistance and static transport number of membranes.

| Polymer | Thickness (μm) | IEC (meg/g dry) | Water content (%) | $R_m$ ($\Omega$ cm$^{-2}$) | $t_-$ ($OH^-$) |
|---|---|---|---|---|---|
| PES-PF-OH | 23 | 1.44 | 15.1 | 17.7 | 0.91 |
| PES-P-OH | 22 | 1.50 | 25.1 | 29.9 | 0.92 |
| PES-E-N | 22 | 1.52 | 25.8 | 28.5 | 0.92 |
| PES-B-OH | 24 | 1.51 | 20.0 | 35.2 | 0.93 |

**Table 4**
The mole fraction of degradation and viscosity values change.

| Polymer | Mole fraction of degradation | | | Viscosity values change | | |
|---|---|---|---|---|---|---|
| | $x$ | $y$ | $x+y$ | Viscosity before testing (dL/g) | Viscosity after testing (dL/g) | Percentage of viscosity change (%) |
| PES-P-OH | 0.14 | 0.08 | 0.22 | 1.13 | 1.02 | 9.7 |
| PES-E-OH | 0.15 | 0.42 | 0.57 | 1.20 | 0.99 | 17.5 |
| PES-PF-OH[a] | – | – | – | 1.15 | 0.25 | 78.3 |
| PES-B-OH | 0.16 | – | 0.16 | 1.15 | 1.08 | 6.1 |

$x$: the mole fraction of degradation caused by substitution reaction. $y$: the mole fraction of degradation caused by Hofmann elimination reaction.

[a] The percent of degradation could not calculate from $^1$H NMR due to overlap of the peaks.

conductivity cells. The measurement was carried out in 0.1 mol $L^{-1}$ NaOH solution. The resistance was calculated by the resistance of conductivity cell subtracting the resistance of electrolyte solutions. The electromotive force ($E$) between both sides of a membrane, which caused by different concentrations, was measured by two reverse Ag/AgCl electrodes connected to an auto voltmeter. The membrane potential is obtained from the difference of $E$ and the standard solution potential $E_0$:

$$E = E - E_0 \text{ and } E_0 = -\frac{RT}{F}\ln\frac{C_2}{C_1} \tag{3}$$

where $R$ is gas constant, $T$ is absolute temperature, $F$ is faraday constant,$C_1$ and $C_2$ are the concentration of aqueous solution in the two sides. The static transport number $t_-$ of the hydroxyl in the membrane is given by Eq. (4):

$$t_- = \frac{2E}{E_0} \tag{4}$$

### 2.3.4. Alkaline stability

The alkaline stability of the membranes was evaluated in 10 M KOH solution at 30 °C. The percentage of degradation ($x$, $y$) was expressed as:

$$x = \frac{M(-\mathrm{N(Me)_2})}{M(-\mathrm{N(Me)_3})};\ y = \frac{M(-\mathrm{CH} = \mathrm{CH_2})}{M(-\mathrm{N(Me)_3})} \tag{5}$$

where $M(-\mathrm{N(Me)_2})$ and $M(-\mathrm{CH} = \mathrm{CH_2})$ are the molar of $-\mathrm{N(Me)_2}$ and $-\mathrm{CH{=}CH_2}$ groups generated by degradation after test in 10 M KOH solution, respectively. $M(-\mathrm{N(Me)_3})$ is the mole of $-\mathrm{N(Me)_3}$ groups in original membranes. The integral values in $^1$H NMR spectra were used in the calculation of $x$ and $y$ values.

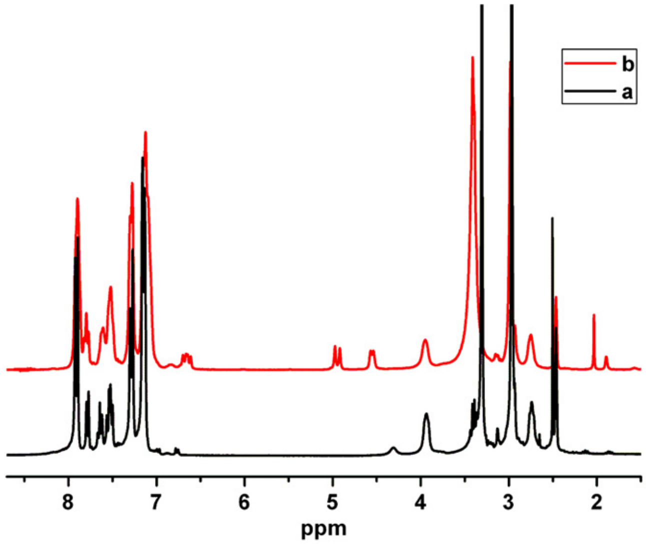

**Fig. 6.** $^1$H NMR spectra of PES-E-OH (a) and PES-E-OH treating with KOH for 24 h (b) in DMSO.

## 3. Results and discussion

### 3.1. Synthesis and characterization of monomers and polymers

The typical synthetic routes for the biphenol monomer (PPH-DMEA) and quternized polymer containing $-[\mathrm{CH_2CH_2NMe_3}]^+\mathrm{OH}^-$ groups, PES-E-OH, were shown in Scheme 1 and 2, respectively. The monomer was synthesized by condensation of phenolphthalein with N,N-dimethylethane-1,2-diamine (DMEA) in the yield of 82% according to the literature method for the synthesis of monomer PPH–DMEA reported by our groups [18]. Polymer containing $-[\mathrm{CH_2CH_2CH_2NMe_3}]^+\mathrm{OH}^-$ groups, PES-P-OH, and partially fluorinated polymer, PES-PF-OH, were prepared from PPH-DMPA and DCDPS, PPH-DMPA and 3,3′,4,4′-tetrafluorodiphenylsulfone, respectively. For the sake of comparison, polymer containing $-[\mathrm{CH_2NMe_3}]^+\mathrm{OH}^-$ groups, PES-B-OH, was prepared according to our previously reported method [19]. All structures of the quaternized polymers in this study were shown in Fig. 1. In a typical procedure for

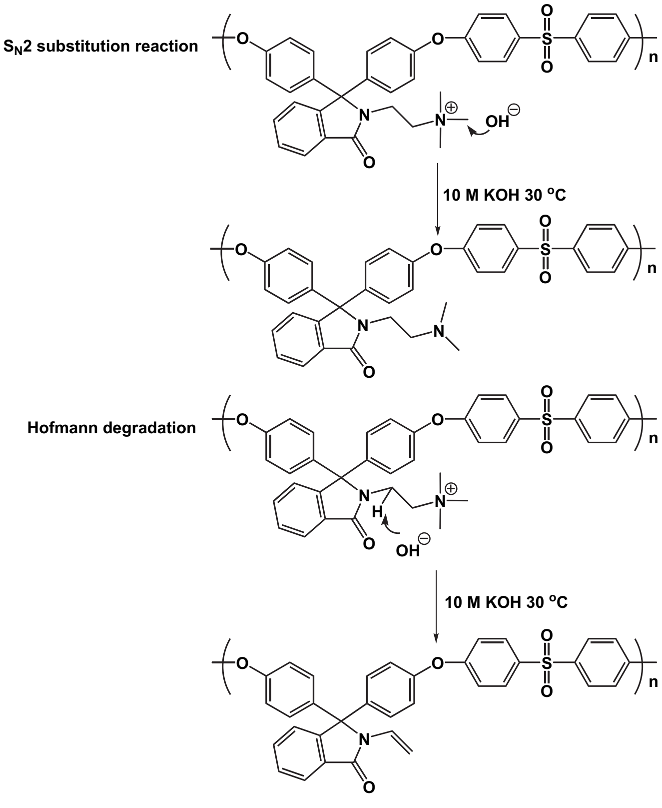

**Scheme 3.** Degradation mechanism of PES-E-OH in KOH solution (10 M) at 30 °C.

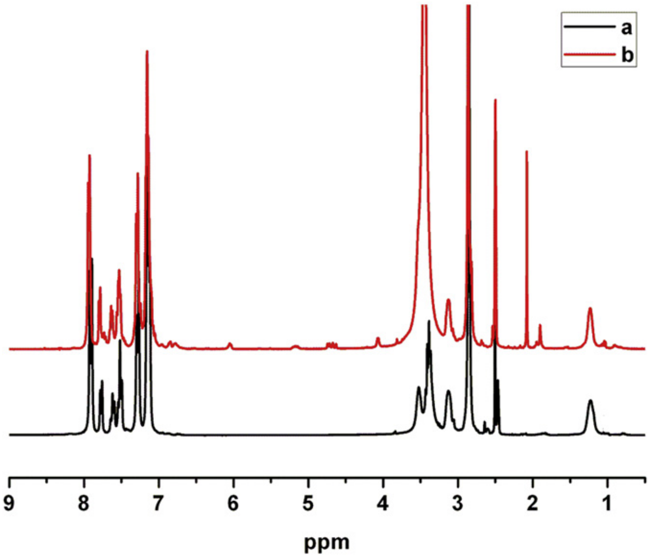

**Fig. 7.** $^1$H NMR spectra of PES-P-OH (a) and PES-P-OH treating with KOH for 24 h (b) in DMSO.

the synthesis of PES-E-N, a stoichiometric ratio of the PPH-DMPA and DCDPS, an excess of potassium carbonate, and NMP with a 20% solid content were used. The reaction was first held at 140 °C for 4 h under nitrogen to azeotrope off water with toluene and then was heated up to 180 °C for 10 h to afford a high-molecular-weight polymer. All polymers containing tertiary amine groups were converted to the quaternized poly(aryl ether sulfone)s by reaction with iodomethane at 20 °C for 24 h. The mole ratio of iodomethane to tertiary amine groups was set to be 2:1 to ensure complete conversion of the tertiary amine units into the quaternary ammonium moieties.

The high-molecular-weight polymers can be successfully synthesized by nucleophilic aromatic substitution polymerization, each of which had high-molecular-weight ($M_n > 40.7 \times 10^3$ g/mol, $M_w > 89.7 \times 10^3$ g/mol), as evidenced by GPC analyses and their high viscosity values (Table 1). These polymers showed good solubility in polar aprotic solvents, such as dimethylacetamide (DMAc), dimethylsulfoxide (DMSO), and NMP. The chemical structures of the polymers were confirmed by FT-IR and $^1$H NMR spectra. Fig. 2 shows the hydrogen signal assignment in the $^1$H NMR spectra of PES-P-OH and PES-PF-OH. Two typical peaks of a tertiary amine group were observed at $\delta$ 1.95 ($-CH_2-$), and 2.19 ($-CH_3$) for PES-P-N and PES-PF-N. After quaternization, proton signals of methylene and methyl were shifted to higher frequencies ($\delta$ 3.14 ($-CH_2-$) and 2.86 ($-CH_3$)) as a result of the deshielding from the quaternary nitrogen atom. The integration ratio of $H_i$ to $H_k$ was close to 9:2, suggesting a quantitative conversion of tertiary amine to ammonium groups. The peak at $\delta$ 7.89–7.92 ppm was attributed to the hydrogen atom ($H_a$) in the ortho position to the sulfone group. The integration ratio of $H_a$ and $H_i$ was very close to 4:9, as expected for the composition of PES-P-OH. FT-IR spectra of PES-PF-OH revealed the vibration bands at 1683 and 724 cm$^{-1}$, which corresponded to the stretch vibration of carbonyl and Ar–F bonds groups, respectively.

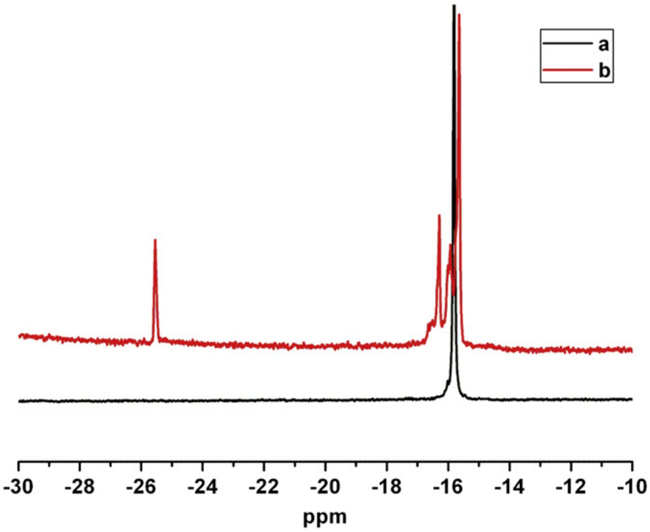

**Fig. 8.** $^{19}$F NMR spectra of PES-PF-OH (a) and PES-PF-OH treating with KOH for 24 h (b) in DMSO.

### 3.2. Thermal and mechanical properties

The thermal stabilities of the membranes were analyzed by recording their TGA curves under flowing nitrogen. The TGA traces of the resulting polymers were presented in Fig. 3 for PES-P-N, PES-P-I and PES-P-OH membranes as representative cases. The tertiary amine polymer PES-P-N was a thermally stable polymer and exhibited the starting decomposition temperature around 260 °C. A two-step degradation profile was observed for the polymer containing $-(CH_2CH_2CH_2NMe_3)^+I^-$ groups (PES-P-I). The first weight loss observed for PES-P-I at 188 °C was assigned to the degradation of the side chain of PES-P-I. The second weight loss region (at temperature >373 °C), the polymer residues were further degraded, corresponded to the decomposition of the main chains of PES-P-I. The polymer containing $-(CH_2CH_2CH_2NMe_3)^+OH^-$ groups (PES-P-OH) showed three-step weight loss. The first weight loss from 128 to 190 °C was due to Hofmann elimination of quaternary ammonium hydroxides. The result indicated that PES-P-OH is less stable than PES-P-I and PES-P-N.

Table 1 lists the mechanical properties of membranes as measured at room temperature and 30% RH. The tertiary amine polymer membranes had tensile strength at maximum load in the range of 50–60 MPa, Young's modulus of 1.08–1.94 GPa, and elongation at break of 10.6–17.9%. After the quaternization, the tensile strength and Young's modulus decreased, and elongation at break improved due to the introduction of strong polar quaternary ammonium moieties in side chains. The quaternized polymer membranes still showed good mechanical properties with tensile strength, elongation at break and Young's modulus in the ranges of 32–48 MPa, 23.8–33.9%, and 0.54–0.86 GPa in dry state, respectively. The tension results showed that they were strong and flexible membrane materials.

### 3.3. IEC, water uptake, and swelling ratio

IEC, water uptake and swelling ratio of membranes were summarized in Table 2. The ion-exchange capacity was determined using the standard back-titration technique reported previously [20]. In all cases, the experimental value of IEC agreed with the theoretical one, demonstrating that I$^-$ ions were completely replaced by OH$^-$ ions.

The water within membranes provides a carrier for the OH$^-$ ions and maintains high OH$^-$ ions conductivity. However, excessive water uptake in AEMs leads to unacceptable dimensional change and loss of dimensional shape. Therefore, the preparation of quaternizated membranes with appropriate water uptake and excellent dimensional stability is one of the critical requirements for their application as AEMs.

The water uptake and swelling ratio of the membranes are reported in Table 2. It could be seen that PES-PF-OH (wu: 15.1%, sr:

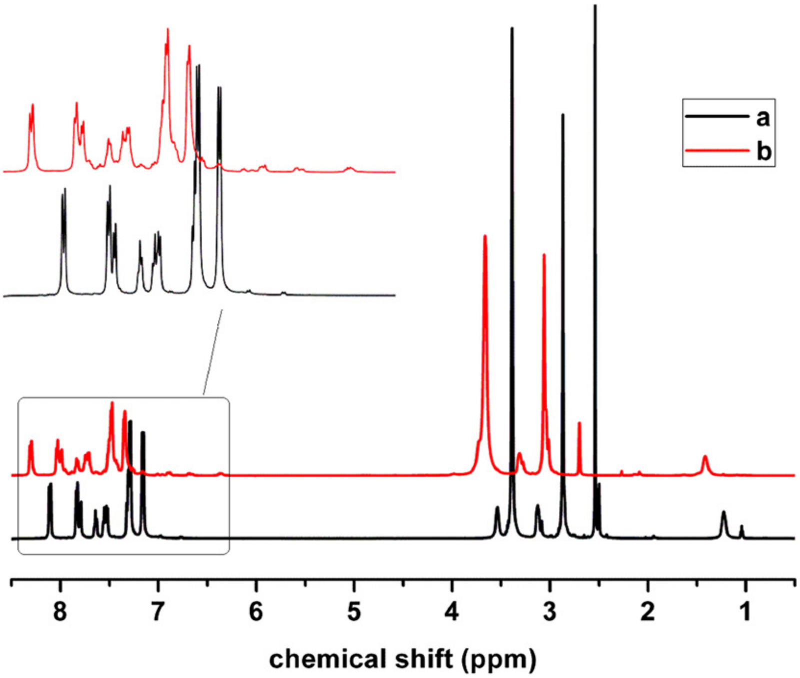

**Fig. 9.** $^1$H NMR spectra of PES-PF-OH (a) and PES-PF-OH treating with KOH for 24 h (b) in DMSO.

2.7% at 20 °C) exhibited a lower water uptake and swelling ratio than those of PES-P-OH (wu: 25.1%, sr: 4.2% at 20 °C) and PES-E-OH (wu: 25.8%, sr: 4.2% at 20 °C), because of more hydrophobic polymer backbone. All of polymers displayed proper water uptake and excellent dimensional stability.

### 3.4. Membrane morphology and hydroxide ion conductivity

Transmission electron micrographs (TEMs) of membranes were shown in Fig. 4. To investigate phase separation and ionic aggregation, membranes were stained with $PdCl_4^{2-}$ anion; thus, dark areas correspond to regions of high ionicity and brighter areas to hydrophobic regions. It was observed that all membranes possessed a phase-separated morphology characterized by ionic clusters. The polymer's chemical structure plays an important role in phase separation and ionic aggregation. Ionic clusters of PES-B-OH (ca. 6–8 nm in diameter) and PES-P-OH (ca. 20–30 nm in diameter) were observed. This morphology is very similar to that of quaternized poly(aryl ether sulfone) reported by Zhuang's group [7], which possesses tens of nanometers ionic clusters. However, after introduction of fluorine into the main chain, the morphology remarkably changed. The ionic cluster size of PES-PF-OH membrane (1–2 nm) shows a substantially decrease and the number density of the ionic clusters demonstrates great increase compared with those of PES-P-OH membrane (Fig. 4d).

The hydroxide ion conductivities of the PES-B-OH, PES-E-OH, PES-P-OH and PES-PF-OH membranes were measured in water in the temperature range of 20–60 °C, and the results were illustrated in Fig. 5. As expected, the hydroxide ion conductivity increased with increasing temperature. All the samples exhibited room temperature conductivities higher than $1 \times 10^{-2}$ S/cm. Hydroxide ion conductivity values for all membranes with similar IEC value ranged between 0.018 and 0.030 S/cm at 20 °C. It can be seen that the order of conductivity is: PES-PF-OH > PES-E-OH ~ PES-P-OH > PES-B-OH. In the entire temperature range studied, PES-PF-OH with the lowest IEC value showed the highest hydroxide ion conductivity compared with other samples. The main chain quaternary ammonia ionomer (PES-B-OH) exhibited a hydroxide conductivity lower than those of others containing pendent quaternary ammonium groups on aliphatic side chains. For instance, as temperature increases from 20 to 60 °C, the conductivity increases from 0.021 to 0.031 S/cm for membrane PES-P-OH (IEC = 1.50 meq g$^{-1}$), from 0.031 to 0.042 S/cm for PES-PF-OH, whereas the conductivity increases steadily from 0.018 to 0.026 S/cm for membrane PES-B-OH (IEC = 1.51 meq g$^{-1}$). The main chain of PES-PF-OH is composed of a partly fluorinated poly(aryl ether sulfone), while the side chain segments containing the ionic groups are composed of flexible, aliphatic chains. The introduction of F atom in the polymer main chain increases the hydrophobicity of the polymer backbone of PES-PF-OH, which facilitates to form hydrophilic/hydrophobic microphase separation

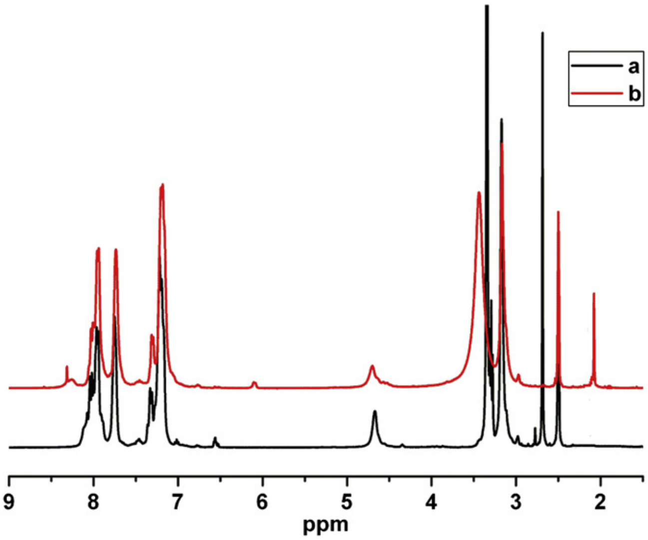

**Fig. 10.** $^1$H NMR spectra of PES-B-OH (a) and PES-B-OH treating with KOH for 24 h (b) in DMSO.

structure. This ultimately results in better-connected ionic domains and high density of ionic clusters leading to the excellent conductivities (Fig. 4d). By combining the microscopic observation and hydroxide conducting behavior, it is concluded that both the size and density of ionic clusters have a great influence on hydroxide conductivity in AEMs.

### 3.5. *Area resistance and static transport number*

In order to further evaluate the practicability for AEMs, area resistance and static transport number were determined and the results were presented in Table 3. Because the thickness of membrane has great effect on area resistance and static transport number, the membranes with the similar thickness were used to test in the experiment. As far as the transport number was concerned, all of them had a value above 0.91. Area resistance of the membranes ranged from 35.2 to 17.7 Ω $cm^2$ and they could also satisfy the requirement for desalination membranes [22]. From Table 3, it can be concluded that the order of area resistance is: PES-B-OH (35.2 Ω $cm^{-2}$) > PES-P-OH (29.9 Ω $cm^{-2}$) ∼ PES-E-OH (28.5 Ω $cm^{-2}$) > PES-PF-OH (17.7 Ω $cm^{-2}$). The sequence is opposite to that of hydroxide ion conductivity. Compared with the PES-B-OH membrane, the PES-P-OH exhibited lower area resistance. This was attributed to more easily form the ion conductive paths through the membrane resulting from ionic groups on the flexible aliphatic side chain of the polymer, which led to the ion migrate through the membrane very easily.

### 3.6. *Alkaline stability of the membranes*

A key property in developing AEMs for fuel cells is the chemical stability of the cationic groups attached to the membrane. Even in an electrochemical cell without any added electrolyte, the localized pH within the ion-conducting channels of membranes will be quite high. High pH can lead to chemical attack on the quaternary ammonium groups and the polymer chain, most commonly by either an E2 (Hofmann degradation) mechanism or an $S_N2$ substitution reaction [23]. In addition, the partially fluorinated copolymer materials were used as AEMs recently, which provided higher ion conductivity [19,24]. But the alkaline stability of these materials has not been investigated. The present section reports the influence of the chemical structures on their alkaline stability.

The alkaline stability of the membranes was evaluated in 10 M KOH solution at 30 °C. The mole fraction of degradation caused by $S_N2$ substitution or Hofmann elimination reactions was denoted as $x$ or $y$, respectively. The values of $x$ or $y$ were calculated by comparing the integral of the signals originating specifically from tertiary amine (2.1 ppm) or alkene groups (4.9 ppm) with the integral of the quaternary ammonium at 2.9 ppm and the results were listed in Table 4.

The $^1H$ NMR spectra of PES-E-OH before and after treatment with 10 M KOH solution at 30 °C for 24 h was given in Fig. 6. Three typical alkene peaks were observed at 4.54–4.57 ppm (d), 4.92–4.97 ppm (d), 6.61–6.70 ppm (q) after test with KOH solution for 24 h and the integration ratio of the three peaks is 1:1:1. The alkene resulted from Hofmann elimination of quaternary ammonium hydroxides, as shown in Scheme 3. Moreover, the quaternary nitrogen atoms are transformed to tertiary nitrogen by $S_N2$ substitution reaction. A proof of this assertion is the presence of the characteristic peak for the tertiary amines at 2.1 ppm in $^1H$ NMR spectra.

The PES-P-OH membrane exhibited a lower $x$ value than that of PES-E-OH (Fig. 7 and Table 4). Compared with PES-P-OH, the poor alkaline stability of PES-E-OH resulted from chemical decomposition by β elimination (Scheme 3). The ease of the abstraction of the proton depends on the electron density at the β-carbon that results from the attachment of electron-withdrawing groups. The electron density at the β-carbon of PES-E-OH is small in comparison to PES-P-OH because of the strong electron-withdrawing effect of nitrogen. The decrease in the electron density at the β-carbon of PES-E-OH makes it easier for the hydroxyl ion to abstract proton. The ease of the β-hydrogen abstraction facilitates decomposition of quaternary ammonium groups to alkene.

The PES-PF-OH membrane breaks into pieces after being treated with 10 M KOH for 24 h. The decomposition of partially fluorinated PES-PF-OH membrane was analyzed by the $^{19}F$ NMR measurements and the $^{19}F$ NMR spectra were shown in Fig. 8. In the $^{19}F$ NMR spectra of the initial membrane, only a single peak attributed to the meta fluorine atoms (relative to the sulfone group) on the main chain was observed at −15.8 ppm. Four new peaks are clearly evident in the $^{19}F$ NMR spectra of the PES-PF-OH after being treated with 10 M KOH for 24 h at −25.6, −16.3, −16.0 and −15.9 ppm. It is concluded that F in the polymer backbone was substituted by hydroxide ion and the main chain of polymer split off. However, $^1H$ NMR spectra (Fig. 9) indicated that $S_N2$ substitution reaction and Hofmann elimination of quaternary ammonium hydroxides did not occur in PES-PF-OH membrane.

Meanwhile, $^1H$ NMR spectra of PES-B-OH (Fig. 10) showed that the degradation caused by $S_N2$ substitution reaction is more significantly than others, demonstrated by the characteristic peak at 2.1 ppm. This was attributed to that the benzyl group was easily substituted by hydroxide ions. However, it can be seen from the data in Table 4 that the PES-B-OH exhibited the lowest mole fraction of degradation ($x + y$), which indicated that PES-B-OH was more stable against hydroxide ions attack compared with other membranes, owing to the lack of Hofmann elimination of quaternary ammonium hydroxides. And PES-PF-OH main chain was the mostly unstable. It was inferred from the above that their alkaline stability in 10 M KOH solution follows the order: PES-B-OH > PES-P-OH > PES-E-OH > PES-PF-OH.

## 4. Conclusion

A series of novel poly(aryl ether sulfone)s that contain pendent quaternary ammonium groups on aliphatic side chains have been prepared as hydroxide ion conductive materials. We demonstrated that using functionalized monomer it is possible to directly obtain different quaternized poly(aryl ether sulfone)s for anion exchange membranes. Compared with traditional approach, this process could precisely control the amount of quaternary ammonium groups and their location along the polymer backbone. Additional, this new route avoided the use of chloromethyl methyl ether-a toxic chemical, and thus it was more environmentally friendly. The obtained quaternized ionomers exhibited excellent solubility and formed flexible and tough membranes by casting from NMP solution. The introduction of hydrophobic fluorine groups in the polymer main chain resulted in the low water uptake, area resistance and the excellent dimensional stability of the PES-PF-OH membranes. It showed high hydroxide conductivity up to $3.0 \times 10^{-2}$ S $cm^{-1}$ in water at 20 °C. All membranes possessed a phase-separated morphology characterized by ionic clusters. The alkaline stability of the membranes was evaluated in 10 M KOH solution at 30 °C, investigated by $^1H$ and $^{19}F$ NMR, and viscosity change. The result shows that PES-B-OH membrane displays better alkaline stability than others. It is observed that the presence of fluorine atoms in the aromatic ring leads to a poor stability in KOH solution.

## Acknowledgements

We thank the National Basic Research Program of China (No. 2009CB623401), the National Science Foundation of China

(Nos.50825302, 50973106), and the Development of Scientific Technological Projects of the Jilin Province (No. 20080620) for financial support.

## References

[1] Carrette I, Friedrich KA, Stimming U. Fuel Cells 2001;1:5–39.
[2] Jacobson MZ, Colella WG, Golden DM. Science 2005;308:1901–5.
[3] Steele BCH, Heinzel A. Nature 2001;414:345–52.
[4] Hickner MA, Chassem H, Kim YS, Einsla BR, McGrath JE. Chem Rev 2004;104:4587–612.
[5] Varcoe JR, Slade RCT, Yee ELH, Poynton SD, Driscoll DJ, Apperley DC. Chem Mater 2007;19:2686–93.
[6] Tanaka M, Koike M, Miyatake K, Watanabe M. Macromolecules 2010;43:2657–9.
[7] Pan J, Lu S, Li Y, Huang A, Zhuang L, Lu J. Adv Funct Mater 2010;20:312–9.
[8] Lu S, Pan J, Huang A, Zhuang L, Lu J. Proc Natl Acad Sci 2008;105:20611–4.
[9] Wang J, Li S, Zhang S. Macromolecules 2010;43:3890–6.
[10] Gu S, Cai R, Luo T, Chen Z, Sun M, Liu Y, et al. Angew Chem Int Ed 2009;48:6499–502.
[11] Wang G, Weng Y, Chu D, Chen R, Xie DJ. Membr Sci 2009;332:63–8.
[12] Blair A, Kazerouni N. Cancer Causes Control 1997;8:473–90.
[13] Laskin S, Kusschner M, Drew RT, Capiello VP, Nelson N. Arch Environ Health 1971;23:135–42.
[14] Norsten TB, Guiver MD, Murphy J, Astill T, Navessin T, Holdcroft S, et al. Adv Funct Mater 2006;16:1814–22.
[15] Lafitte B, Jannasch P. Adv Funct Mater 2007;17:2823–34.
[16] Seesukphronrarak S, Ohira A. Chem Commun; 2009:4744–6.
[17] Zhang Q, Zhang S, Dai L, Chen XJ. Membr Sci 2010;349:217–24.
[18] Zhang Q, Zhang Q, Zhang S, Li SJ. Membr Sci 2010;354:23–31.
[19] Wang J, Zhao Z, Gong F, Li S, Zhang S. Macromolecules 2009;42:8711–7.
[20] Slade RCT, Varcoe JR. Solid State Ionics 2005;176:585–97.
[21] Li X, Wang Z, Lu H, Zhao C, Na H, Zhao CJ. Membr Sci 2005;254:147–55.
[22] Cheng S, Sun B, Li W, Wu G. Membr Sci Technol 1998;18:34–7.
[23] Hibbs MR, Fujimoto CH, Cornelius CJ. Macromolecules 2009;42:8316–21.
[24] Valade D, Boschet F, Roualdè S, Ameduri B. J Polym Sci Part A Polym Chem 2009;47:2043–58.